Benha Journal of Applied Sciences (BJAS) **print: ISSN 2356–9751**
Vol. (9) Issue (6) (2024), (1-7) **online: ISSN 2356–976x**
http://bjas.bu.edu.eg

Hydrothermal synthesis of vanadium disulfide: Experimental optimization and characterization

Mona S. NourEldien [1*], Mostafa Y. Nassar[1,2], Islam M. Ibrahim[1] and Hisham M. Aly[1]
[1]Department of Chemistry, Faculty of Science, Benha University, Benha 13518, Egypt.
[2]Department of Chemistry, College of Science, King Faisal University, P.O. Box 400, Al-Ahsa 31982, Saudi Arabia.
E-mail: mona.noureldin@fsc.bu.edu.eg

Graphical abstract

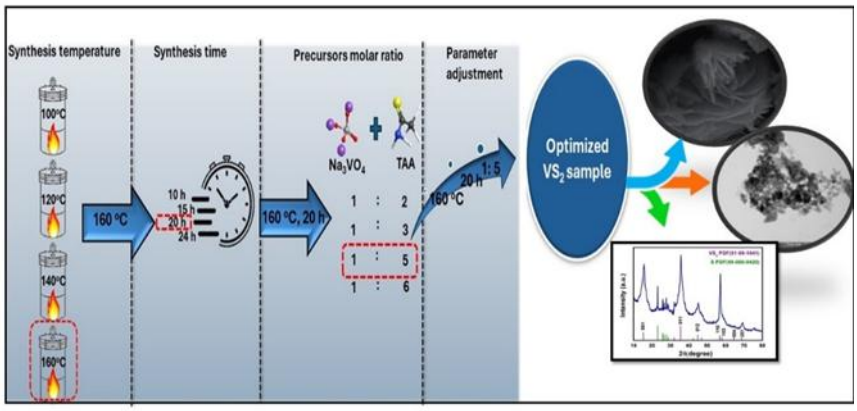

Abstract

Vanadium disulfide (VS_2) nanosheets (NS) have garnered significant attention due to their unique structural and electronic properties, making them suitable for various advanced applications. This work investigates the optimization of hydrothermal synthesis parameters to produce high-quality VS_2 nanosheets. Key synthesis variables, including temperature, reaction time, and precursor concentrations, were systematically varied to assess their impact on the structural, and morphological of the resulting nanosheets. Characterization techniques such as X-ray diffraction (XRD), scanning electron microscopy (SEM), and transmission electron microscopy (TEM) were employed to analyze the crystalline structure and morphology of the prepared VS_2 nanosheets. The optimized synthesis conditions resulted in the formation of VS_2 nanosheets with enhanced crystallinity, confirming a layered hexagonal crystal structure with lattice parameters of a = b = 3.2210 Å and c = 5.7550 Å. The SEM images demonstrate the distinct nanoflower structure of VS_2, which was not evident in non-optimized samples This study underscores the importance of precise control over synthesis parameters to achieve desired material properties.

Keywords: VS_2 nanosheets; Hydrothermal synthesis; Optimization.

1. Introduction

Two-dimensional single and few-layered transition metal dichalcogenides (TMDs) have gained popularity due to their strong in-plane bonding and comparatively weak out-of-plane bindings. These materials exhibit amazing characteristics such as their single or multiple layers, extraordinary flexibility, the absence of dangling bonds caused by van der Waals pressures, and more [1-3]. These materials can exist in several states, such as semiconductor, insulator, semi-metal, and true-metal structures, depending on their oxidation states and coordination [3]. The desirable electronic and magnetic properties can be obtained by carefully controlling the compositional variation, functionalization, and application of external fields [4]. Most 2D materials are naturally non-magnetic in their original state. However, the layered composition of 2D transition metal dichalcogenides (TMDs) and their various structural phases have bestowed them with exceptional material properties, making them ideal for use in logic circuits, field-effect transistors, light-emitting diodes, photodetectors, and similar applications [4]. These TMD layers are found in the form of sandwich structures, where the transition metals (groups 4–10) are sandwiched between chalcogen atoms (X: S, Se, and Te) [5-7].

The remarkable electrical, electrochemical, magnetic, and optical features of VS_2 nanomaterials have attracted significant attention among researchers studying Transition Metal Dichalcogenides (TMDs) [8-11]. The two-dimensional structure of these materials is usually one or two layers thick, much like other transversely sandwiched atomic layers held together by van der Waals interaction [12]. The exceptional characteristics of 2D TMD VS_2,

including its electrical configuration, structural layout, bandgap, and van der Waals interactions [13, 14], render it well-suited for comprehensive investigation from a basic standpoint. Paying close attention to these characteristics while synthesizing VS_2 nanomaterials should provide a more accurate result, enabling substantial property modification. Experimental methodologies and techniques impact different underlying mechanisms, which in turn affect the properties following synthesis, beyond these basic aspects. Among various synthesis methods, the hydrothermal approach for producing VS_2 has gained significant attention. This method is favored due to its simplicity, energy efficiency, and cost-effectiveness. The hydrothermal synthesis process allows for precise control over the reaction conditions, leading to high-quality VS_2 with desirable properties for various applications [15-17].

This research breaks new ground by focusing on the optimization of the hydrothermal synthesis of VS_2 nanosheets, a material with promising potential. By systematically varying synthesis parameters, we seek to comprehensively understand their effects on the morphological and structural properties of VS_2 nanosheets. The identification of optimal synthesis conditions will be achieved through an integrated approach using advanced characterization techniques, X-ray diffraction (XRD), scanning electron microscopy (SEM), and transmission electron microscopy (TEM). This study's novelty lies in its detailed exploration of how synthesis parameters influence the properties of VS_2 nanosheets, paving the way for advancements in their applications.

2. Materials and methods

All chemicals used in this research were obtained from commercial suppliers and were not further processed from their original forms. Throughout the trials, deionized (DI) water was utilized for both the solvent and washing purposes.

2.1 Synthesis of VS_2 nanosheets

In a typical synthesis, VS_2 nanosheets were prepared using a cost-effective hydrothermal method [18], by reacting sodium orthovanadate (Na_3VO_4) with thioacetamide (TAA). Specifically, 0.112 g of TAA and 0.055 g of Na_3VO_4 were dissolved in 40 mL of deionized water and stirred magnetically for 1 hour to form a homogeneous solution. This solution was then transferred into a 100 mL Teflon-lined stainless-steel autoclave, sealed, and heated at 160 °C for 20 hours. After cooling, the product was washed several times with ethyl alcohol and deionized water. The resulting black powder was then dried in an electric oven at 80 °C for 10 hours. Moreover, to further investigate optimizing the synthesized products, a series of experiments with systematic variations in hydrothermal synthesis were conducted, as shown in **Fig. 1**. The adjustments included changing the reaction temperature, the reaction duration, and the molar ratio of precursors as detailed below.

2.1.1 Optimization with Respect to Reaction Temperature

This set of samples, referred to as the temperature-group, was utilized to investigate the impact of different hydrothermal temperatures (T_s = 100 °C, 120 °C, 140 °C, and 160 °C), while maintaining other experimental conditions constant. The solution consisted of 0.055 g Na_3VO_4, 0.112 g TAA, and 40 ml H_2O, keeping the molar ratio of TAA to Na_3VO_4 at 5, with a hydrothermal treatment duration of 20 hours.

2.1.2 Optimization with Respect to Reaction Time

This set of samples, referred to as the time-group, was employed to examine the effects of different hydrothermal times (t_s = 24 h, 20 h, 15 h, and 10 h), with other experimental conditions remaining fixed. The solution contained 0.055 g Na_3VO_4, 0.112 g TAA, and 40 ml H_2O, maintaining the molar ratio of TAA to Na_3VO_4 at 5. The mixed solution was subjected to hydrothermal treatment at 160°C.

2.1.3 Optimization with Respect to Precursors Molar Ratio

This set of samples, known as the ratio-group, was used to explore the effects of various ratios of precursors (Na_3VO_4: TAA) [(1:2), (1:3), (1:5), (1:6)], while keeping other experimental conditions constant. The solution comprised 0.055 g Na_3VO_4, 0.112 g TAA, and 40 ml H_2O. The mixed solution underwent hydrothermal treatment at 160°C for 20 hours.

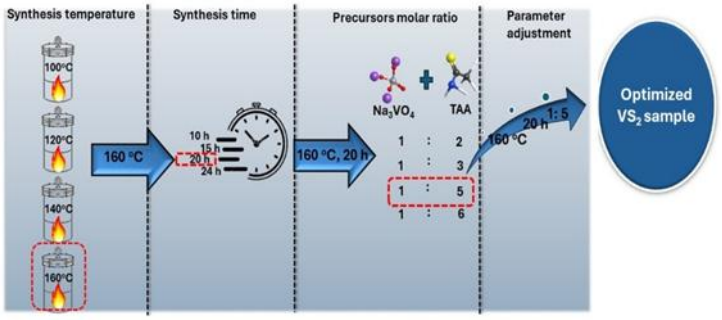

Fig. (1) Schematic procedures for obtaining an optimal VS_2 sample.

2.2 Characterization

Various methodologies were employed to conduct the structural examination of the initial samples. The X-ray diffraction (XRD) analysis was performed using a Bruker model D8 Advance equipment equipped with Cu-Kα radiation and a step interval of 0.02^o. The morphological analysis was conducted using field emission scanning electron microscopy (FE-SEM) at an operating voltage of 30 kV, and high-resolution transmission electron microscopy (HR-TEM) using a JEM-2100 apparatus at 200 kV.

3. Results and discussion

3.1 XRD of VS_2 samples

XRD analysis was utilized to investigate the crystalline structures of various VS_2 sample groups. The crystallite size (D) was determined by the Debye-Scherer Eq. 1 [19], and shown in **Table 1**,

$$D = \frac{k\lambda}{B\cos\theta} \quad (1)$$

Where θ represents the diffraction angle, K is a constant set at 0.9, and β denotes the full width at half maximum (FWHM).

3.1.1 Optimization with respect to reaction temperature

The XRD patterns in **Fig. 2(a)** illustrate the impact of temperature on the samples categorized by temperature groups. Temperature plays a crucial role in determining particle size, as summarized in **Table 1**. It influences both particle growth and crystallization. **Figure 2** shows that the XRD patterns of samples treated at reactive temperatures of 100, 120, and 140°C are predominantly amorphous in the range of 2θ=20 to 80 degrees. Notably, a distinct peak at 2θ = 15.6 is visible in these samples, corresponding to the (0 0 1) lattice plane of VS_2 nanosheets. Upon increasing the hydrothermal temperature to 160°C, the XRD peak intensities for VS_2 become stronger, and the XRD diffraction peaks become slightly narrower, indicating the formation of larger and more crystalline VS_2 particles and an enhancement in crystallization. This observation suggests that hydrothermal treatment promotes the phase transition of VS_2 from amorphous to crystalline. The most favorable XRD outcomes are achieved at 160°C.

3.1.2 Optimization with respect to reaction time

Figure 2(b) displays the XRD patterns of Time-group samples synthesized at 160°C. Time significantly impacts particle size, as evidenced by **Table 1**, which presents the average crystalline sizes of VS_2 samples prepared at 160°C across various hydrothermal treatment durations. The data indicate that prolonged hydrothermal treatment leads to increased peak intensities and a narrower (0 1 1) plane diffraction peak of VS_2 (2θ = 35.6). This trend reflects the growth in average crystalline sizes and relative VS_2 crystallinity with longer hydrothermal durations, attributed to the promotion of Ostwald ripening [20]. It can be seen that the best XRD results are obtained at at 20 h reaction time.

3.1.2 Optimization with respect to molar ratio of precursors

The results from the Ratio-group samples are illustrated in **Fig. 2(c)**, with the particle size variation detailed in Table 3-1. At a molar ratio of 1: 3, only one peak at 2θ = 15.6 corresponds to the (0 0 1) lattice plane of VS_2 NS. Increasing the molar ratio to 1:4 reveals the presence of a peak for the (0 1 1) plane, indicating VS_2 NS growth. Subsequent increases to molar ratios of 1: 5 and 1: 6 result in sharper and more intense peaks, with additional peaks at 2θ = 57.1, 69.4, and 69.2 corresponding to hexagonal VS_2 NS. This trend suggests that higher V^{4+}: S^{2-} molar ratios lead to smaller particle sizes, attributed to a reduction in reactive velocity due to decreased effective precursor concentrations [21].

So, the best sample of VS_2 NS is obtained with a hydrothermal reaction of Na_3VO_4 and TAA at 160°C for 20 hours with a molar ratio of 1: 5 with the provided XRD pattern in Fig. 3(d). The analysis confirmed that the VS_2 has a layered hexagonal crystal structure, with lattice parameters a = b = 3.2210 Å and c = 5.7550 Å, as indicated by the matching diffraction peaks (lattice planes) in the optimized sample and the data from JCPDS card 01-089-1640 [22]. The prominent peak at 35.6° indicates crystal growth in the (011) lattice plane, aligning with the TEM observations. The XRD peaks between 20° and 30° 2θ match the JCPDS line spectrum (98-000-0420), suggesting the presence of elemental sulfur (S), likely due to sulfur ion reduction caused by a small amount of TAA impurities in the pores of VS_2 [23, 24].

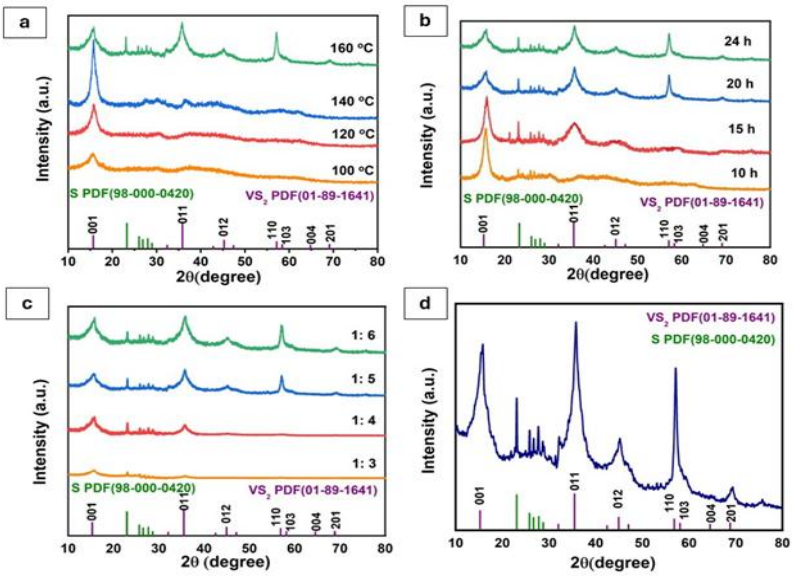

Fig. (2) XRD of VS_2 samples, (a) Temperature-group; (b) Time-group; (c) Ratio-group and (d) the optimized VS_2 sample.

Table (1) The average crystallite size (D) of VS_2 samples synthesized under different conditions.

Group	**Condition**			
Temperature-group samples	100 °C	120 °C	140 °C	160 °C
	Avg. Crystallite size D (nm)			
	3.57	3.46	7.19	20.98
Time-group samples	10 h	15 h	20 h	24 h
	Avg. Crystallite size D (nm)			
	6.06	11.41	20.98	22.76
Ratio-group samples	1: 3	1: 4	1: 5	1: 6
	Avg. Crystallite size D (nm)			
	7.03	12.7	20.98	25.34

3.2 Surface morphology

The samples' morphology was examined using field-emission scanning electron microscopy (FE-SEM) and high-resolution transmission electron microscopy (HR-TEM). **Figures 3(a)** and **3(b)** illustrate low-magnification FE-SEM images of the optimized VS_2, showing a flower-like microstructure made up of nanosheets stacked randomly. The high-resolution SEM image (**Fig. 3(c)** and **3(d)**) offers a detailed view of these nanosheet layers, which are around 46 nm thick and oriented randomly. To provide a comparison of VS_2 morphology, SEM images of one sample from each synthesized group are shown in Fig. 4. These images reveal that the nanosheet structure of VS_2, particularly arranged in a nanoflower shape, is not evident in the selected non-optimized samples.

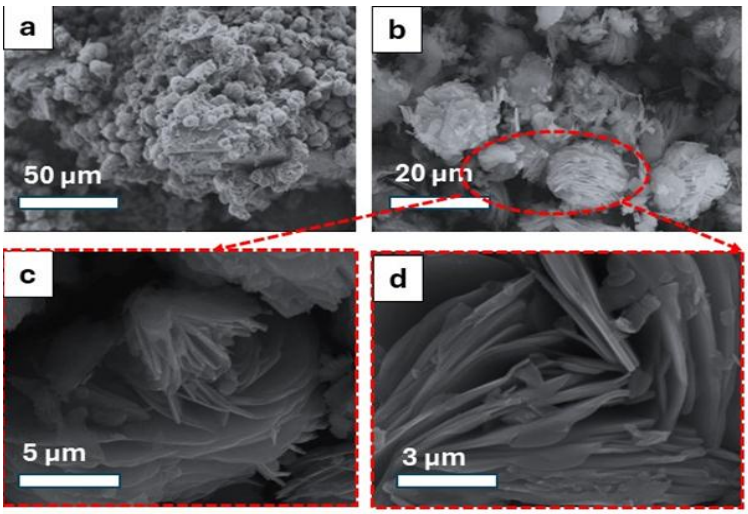

Fig. (3) (a &b) Low magnification SEM images and (c & d) high magnification SEM images of the optimized VS_2 sample.

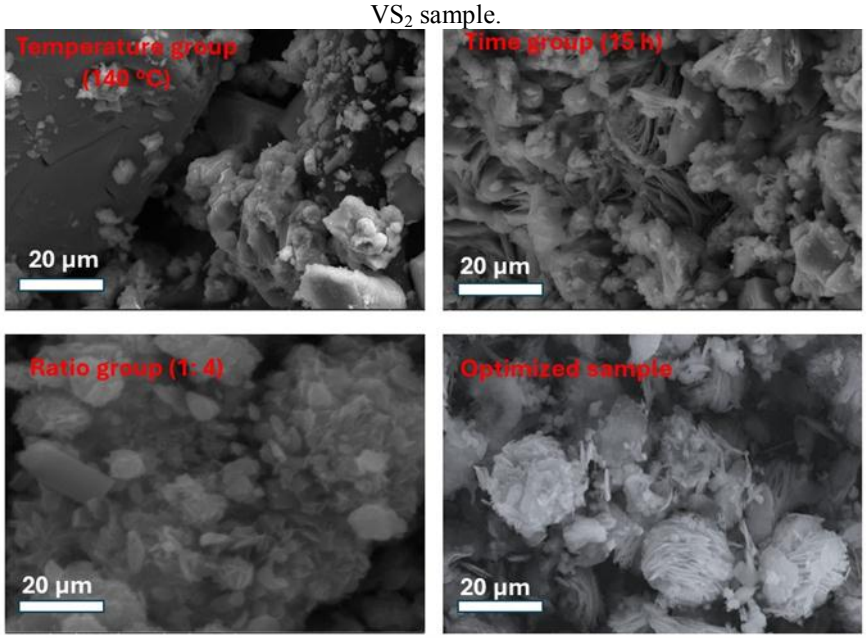

Fig. (4) Comparison of the morphology of selected as-Prepared samples via SEM analysis.

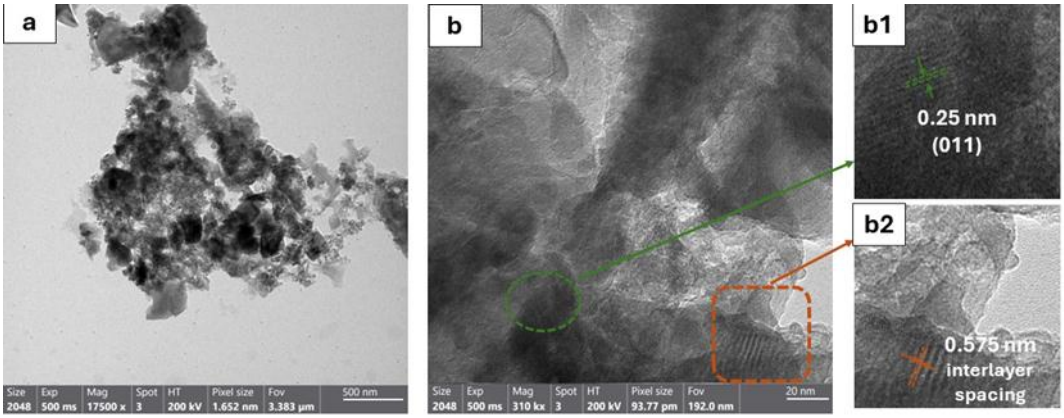

Fig. (5) (a&b) TEM/HR-TEM images of VS_2 at different magnifications; highlighted regions of (b) show the lattice spacing of VS_2 (b1), and an interlayer spacing (b2).

Transmission electron microscopy (TEM) analysis was conducted on the optimized VS_2 sample at various magnifications to validate their microstructures. **Figure 5(a)** depicts a TEM image revealing the hierarchical arrangement of VS_2, composed of nanosheet-like structures. The high-resolution TEM (HRTEM) image in **Fig. 5(b)** highlights an interlayer spacing of 0.575 nm between adjacent monolayers, corresponding to the (001) interlayer spacing along the c-axis direction of pristine VS_2 nanosheets [25]. The other highlighted area shows a periodic lattice fringe pattern with an interplanar spacing "d" of 0.25 nm corresponding to the (011) crystal plane VS_2 [26].

Conclusion

The hydrothermal synthesis of vanadium disulfide (VS_2) has been investigated comprehensively in this study, focusing on experimental optimization and characterization aspects. Through systematic variation of synthesis parameters, we have gained insights into their effects on the morphological, structural, and electronic properties of VS_2. Our findings, supported by advanced characterization techniques such as X-ray diffraction (XRD), scanning electron microscopy (SEM), and transmission electron microscopy (TEM), have led to the determination of the ideal synthesis conditions for VS_2 nanosheets involved a setup at 160°C for 20 hours, with a molar ratio of 1: 5 for V and S source, respectively. Notably, the SEM images demonstrate the distinct nanoflower structure of VS_2, which was not evident in non-optimized samples. These results contribute significantly to the understanding of VS_2 synthesis

and lay a solid foundation for further exploration of its applications in various fields.

Funding
This research received no external funding.

Conflicts of Interest
The authors declare no conflict of interest.

Ethical approval
Institutional Review Board Statement: The study was conducted and approved according to the guidelines of the declaration of the ethical committee of the Faculty of Science, Benha University (No. BUFS-REC-2024-208 Chm).

References

[1] S. Tian, Q. Tang, Activating transition metal dichalcogenide monolayers as efficient electrocatalysts for the oxygen reduction reaction via single atom doping, J. Mater. Chem. C, 9 (2021) 6040-6050.
[2] J. Zhang, S. Liu, H. Liang, R. Dong, X. Feng, Hierarchical Transition-Metal Dichalcogenide Nanosheets for Enhanced Electrocatalytic Hydrogen Evolution, Adv Mater., 27 (2015) 7426-7431.
[3] Q. Lu, Y. Yu, Q. Ma, B. Chen, H. Zhang, 2D transition□ metal□ dichalcogenide□ nanosheet□ based composites for photocatalytic and electrocatalytic hydrogen evolution reactions, Adv. Mater., 28 (2016) 1917-1933.
[4] M. Wu, Y. Xiao, Y. Zeng, Y. Zhou, X. Zeng, L. Zhang, W. Liao, Synthesis of two□ dimensional transition metal dichalcogenides for electronics and optoelectronics, InfoMat, 3 (2021) 362-396.
[5] T. Chowdhury, E.C. Sadler, T.J. Kempa, Progress and prospects in transition-metal dichalcogenide research beyond 2D, Chem. Rev., 120 (2020) 12563-12591.
[6] M. Samadi, N. Sarikhani, M. Zirak, H. Zhang, H.-L. Zhang, A.Z. Moshfegh, Group 6 transition metal dichalcogenide nanomaterials: synthesis, applications and future perspectives, Nanoscale Horiz., 3 (2018) 90-204.
[7] A. Ciarrocchi, A. Avsar, D. Ovchinnikov, A. Kis, Thickness-modulated metal-to-semiconductor transformation in a transition metal dichalcogenide, Nat. Commun., 9 (2018) 919.
[8] X. Zhang, Q. He, X. Xu, T. Xiong, Z. Xiao, J. Meng, X. Wang, L. Wu, J. Chen, L. Mai, Insights into the Storage Mechanism of Layered VS_2 Cathode in Alkali Metal□ Ion Batteries, Adv. Energy Mater., 10 (2020) 1904118.
[9] X. Yu, M.S. Prévot, N. Guijarro, K. Sivula, Self-assembled 2D WSe_2 thin films for photoelectrochemical hydrogen production, Nat. Commun., 6 (2015) 7596.
[10] J. Feng, L. Peng, C. Wu, X. Sun, S. Hu, C. Lin, J. Dai, J. Yang, Y. Xie, Giant moisture responsiveness of VS_2 ultrathin nanosheets for novel touchless positioning interface, Adv. Mater., 15 (2012) 1969-1974.
[11] J. Zhou, L. Wang, M. Yang, J. Wu, F. Chen, W. Huang, N. Han, H. Ye, F. Zhao, Y. Li, Hierarchical VS_2 nanosheet assemblies: a universal host material for the reversible storage of alkali metal ions, Adv. Mater., 29 (2017) 1702061.
[12] E. Chen, W. Xu, J. Chen, J. Warner, 2D layered noble metal dichalcogenides (Pt, Pd, Se, S) for electronics and energy applications, Mater. Today Adv., 7 (2020) 100076.
[13] W. He, X. Zheng, J. Peng, H. Dong, J. Wang, W. Zhao, Mo-dopant-strengthened basal-plane activity in VS2 for accelerating hydrogen evolution reaction, J. Chem. Eng., 396 (2020) 125227.
[14] A. Joseph, P. Aneesh, Efficient degradation of methylene blue: A comparative study using hydrothermally synthesised SnS_2, WS_2 and VS_2 nanostructures, Mater. Res. Bull., 146 (2022) 111623.
[15] C. Zhen, B. Zhang, Y. Zhou, Y. Du, P. Xu, Hydrothermal synthesis of ternary $MoS_{2x}Se_{2(1-x)}$ nanosheets for electrocatalytic hydrogen evolution, Inorg. Chem. Front., 5 (2018) 1386-1390.
[16] M.-R. Gao, Y.-F. Xu, J. Jiang, S.-H. Yu, Nanostructured metal chalcogenides: synthesis, modification, and applications in energy conversion and storage devices, Chemical Society Reviews, 42 (2013) 2986-3017.
[17] Z. Liu, Z. Gao, Y. Liu, M. Xia, R. Wang, N. Li, Heterogeneous nanostructure based on 1T-phase MoS_2 for enhanced electrocatalytic hydrogen evolution, ACS Appl. Mater. Interfaces, 9 (2017) 25291-25297.
[18] M. Bhosale, G. Palanisamy, K. Selvakumar, S. Thangarasu, T.-H. Oh, 2D layers of interconnected reduced graphene oxide with vanadium disulfide photocatalysts for Rhodamine B degradation, J. Alloys Compd., 969 (2023) 172350.
[19] Bhawna, R. Sharma, S. Kumar, R. Kumar, P.K. Sahu, V. Kumari, A.K. Mishra, V. Kumar, Unlocking the Potential of N-Doped SnO_2 for Sustainable Photocatalytic Degradation of Carcinogenic Dyes, Separations, 10 (2023) 322.
[20] J.D. Ng, B. Lorber, J. Witz, A. Théobald-Dietrich, D. Kern, R. Giegé, The crystallization of biological macromolecules from precipitates: evidence for Ostwald ripening, J. Cryst. Growth, 168 (1996) 50-62.

[21] H. Li, H.-z. Wu, G.-x. Xiao, Effects of synthetic conditions on particle size and magnetic properties of $NiFe_2O_4$, Powder Technol., 198 (2010) 157-166.

[22] J. Wen, T. Jiang, S. Arken, Selective leaching of vanadium from vanadium-chromium slag using sodium bicarbonate solution and subsequent in-situ preparation of flower-like VS_2, Hydrometallurgy, 198 (2020) 105498.

[23] V.K. Singh, U.T. Nakate, P. Bhuyan, J. Chen, D.T. Tran, S. Park, Mo/Co doped 1T-VS_2 nanostructures as a superior bifunctional electrocatalyst for overall water splitting in alkaline media, J. Mater. Chem. A., 10 (2022) 9067-9079.

[24] D. Wu, C. Wang, M. Wu, Y. Chao, P. He, J. Ma, Porous bowl-shaped VS_2 nanosheets/graphene composite for high-rate lithium-ion storage, J. Energy Chem., 43 (2020) 24-32.

[25] J. Zhang, C. Zhang, Z. Wang, J. Zhu, Z. Wen, X. Zhao, X. Zhang, J. Xu, Z. Lu, Synergistic interlayer and defect engineering in VS_2 nanosheets toward efficient electrocatalytic hydrogen evolution reaction, Small, 14 (2018) 1703098.

[26] W.A. Haider, M. Tahir, L. He, W. Yang, A. Minhas-khan, K.A. Owusu, Y. Chen, X. Hong, L. Mai, Integration of VS_2 nanosheets into carbon for high energy density micro-supercapacitor, J. Alloys Compd., 823 (2020) 151769.